# Excitation of two-colored temporal solitons in a segmented quasi-phase-matching structure

**Xianglong Zeng, [1*] Satoshi Ashihara, [2, 3] Zijie Wang, [1] Tingyun Wang, [1] Yuping Chen, [4] Myoungsik Cha [5]**

[1]*Key Laboratory of Specialty Fiber Optics and Optical Access Networks, SCIE, Shanghai University, Shanghai 200072, China*
[2]*Department of Applied Physics, Faculty of Engineering, Tokyo University of Agriculture and Technology, 2-24-16 Nakacho, Koganei Tokyo 184-8588, Japan*
[3]*PRESTO, Japan Science and Technology Agency (JST), 4-1-8 Honcho, Kawaguchi-shi, Saitama 332-0012 Japan*
[4]*Department of Physics, Shanghai Jiao Tong University, Shanghai 200240, China*
[5]*Department of Physics, Pusan National University, Busan 609-735, Korea*

**Abstract:** We conducted a numerical study on the excitation of a two-colored temporal soliton in a segmented quasi-phase-matching (QPM) structure. The device has three parts: a periodic QPM grating for second-harmonic generation, a single domain for phase shift, and a periodic QPM grating for soliton evolution. The second harmonic pulse generated in the first grating works as a seed in the cascaded up-and-down conversions in the second grating. The numerical results showed that the second harmonic seeding enables the excitation of soliton pulses with an improved spatio-temporal intensity profile in a broad bandwidth of the wave-vector mismatch.



**OCIS codes:** (190.5530) Pulse propagation and temporal solitons; (190.7110) Ultrafast nonlinear optics; (320.5520) Pulse compression

## References and links

1. G. I. Stegeman, D. J. Hagan, and L. Torner, "$\chi^{(2)}$ Cascading Phenomena and Their Applications to All-Optical Signal Processing, Mode-Locking, Pulse Compression and Solitons," J. Opt. Quant. Electron. **28**(12), 1691–1740 (1996).
2. F. W. Wise, L. Qian, and X. Liu, "Applications of cascaded quadratic nonlinearities to femtosecond pulse generation," J. Nonlinear Opt. Phys. Mater. **11**(3), 317–338 (2002).
3. X. Liu, L. J. Qian, and F. Wise, "High-energy pulse compression by use of negative phase shifts produced by the cascade $\chi^{((2))}$:$\chi^{((2))}$ nonlinearity," Opt. Lett. **24**(23), 1777–1779 (1999).
4. S. Ashihara, J. Nishina, T. Shimura, and K. Kuroda, "Soliton compression of femtosecond pulses in quadratic media," J. Opt. Soc. Am. B **19**(10), 2505–2510 (2002).
5. J. Moses, and F. W. Wise, "Soliton compression in quadratic media: high-energy few-cycle pulses with a frequency-doubling crystal," Opt. Lett. **31**(12), 1881–1883 (2006).
6. J. Moses, E. Alhammali, J. M. Eichenholz, and F. W. Wise, "Efficient high-energy femtosecond pulse compression in quadratic media with flattop beams," Opt. Lett. **32**(17), 2469–2471 (2007).
7. M. Bache, J. Moses, and F. W. Wise, "Scaling laws for soliton pulse compression by cascaded quadratic nonlinearities," J. Opt. Soc. Am. B **24**(10), 2752–2762 (2007).
8. C. Menyuk, R. Schiek, and L. Torner, "Solitary waves due to $\chi^{(2)}$:$\chi^{(2)}$ cascading," J. Opt. Soc. Am. B **11**(12), 2434–2443 (1994).
9. P. Di Trapani, D. Caironi, G. Valiulis, D. Danielius, and A. Piskarskas, "Observation of temporal solitons in second-harmonic generation with tilted pulses," Phys. Rev. Lett. **81**(3), 570–573 (1998).
10. X. Liu, L. J. Qian, and F. W. Wise, "Generation of optical spatiotemporal solitons," Phys. Rev. Lett. **82**(23), 4631–4634 (1999).
11. N. E. Yu, J. H. Ro, M. Cha, S. Kurimura, and T. Taira, "Broadband quasi-phase-matched second-harmonic generation in MgO-doped periodically poled LiNbO_3 at the communications band," Opt. Lett. **27**(12), 1046–1048 (2002).
12. S. Ashihara, T. Shimura, and K. Kuroda, "Group-velocity matched second-harmonic generation in tilted quasi-phase-matched gratings," J. Opt. Soc. Am. B **20**(5), 853–856 (2003).
13. S. Ashihara, T. Shimura, K. Kuroda, N. E. Yu, S. Kurimura, K. Kitamura, M. Cha, and T. Taira, "Optical pulse compression using cascaded quadratic nonlinearities in periodically poled lithium niobate," Appl. Phys. Lett. **84**(7), 1055–1057 (2004).
14. X. L. Zeng, S. Ashihara, N. Fujioka, T. Shimura, and K. Kuroda, "Adiabatic compression of quadratic temporal solitons in aperiodic quasi-phase-matching gratings," Opt. Express **14**(20), 9358–9370 (2006).

#113385 - $15.00 USD Received 8 Jul 2009; revised 16 Aug 2009; accepted 1 Sep 2009; published 8 Sep 2009

15. X. Zeng, S. Ashihara, X. Chen, T. Shimura, and K. Kuroda, "Two-color pulse compression in aperiodically poled lithium niobate," Opt. Commun. **281**(17), 4499–4503 (2008).
16. L. Torner, C. Balslev Clausen, and M. M. Fejer, "Adiabatic shaping of quadratic solitons," Opt. Lett. **23**(12), 903–905 (1998).
17. W. E. Torruellas, Z. Wang, D. J. Hagan, E. W. VanStryland, G. I. Stegeman, L. Torner, and C. R. Menyuk, "Observation of two-dimensional spatial solitary waves in a quadratic medium," Phys. Rev. Lett. **74**(25), 5036–5039 (1995).
18. S. Polyakov, H. Kim, L. Jankovic, G. Stegeman, and M. Katz, "Weak beam control of multiple quadratic soliton generation," Opt. Lett. **28**(16), 1451–1453 (2003).
19. S. Carrasco, L. Torner, J. P. Torres, D. Artigas, E. Lopez-Lago, V. Couderc, and A. Barthelemy, "Quadratic Solitons: Existence Versus Excitation," IEEE J. Sel. Top. Quantum Electron. **8**(3), 497–505 (2002).
20. P. Di Trapani, G. Valiulis, A. Piskarskas, O. Jedrkiewicz, J. Trull, C. Conti, and S. Trillo, "Spontaneously generated X-shaped light bullets," Phys. Rev. Lett. **91**(9), 093904 (2003).
21. D. Zelmon, D. Small, and D. Jundt, "Infrared corrected Sellmeier coefficients for congruently grown lithium niobate and 5 mol. magnesium oxide doped lithium niobate," J. Opt. Soc. Am. B **14**(12), 3319–3322 (1997).
22. I. Shoji, T. Kondo, A. Kitamoto, M. Shirane, and R. Ito, "Absolute scale of second-order nonlinear-optical coefficients," J. Opt. Soc. Am. B **14**(9), 2268–2294 (1997).
23. R. DeSalvo, A. A. Said, D. J. Hagan, E. W. Stryland, and M. Sheik-Bahae, "Infrared to ultraviolet measurements of two-photon absorption and $n_2$ in wide bandgap solids," IEEE J. Quantum Electron. **32**(8), 1324–1333 (1996).

## 1. Introduction

A large nonlinear phase shift can be induced on a fundamental frequency (FF) wave through cascaded $\chi^{(2)}$ interactions under phase-mismatched second harmonic generation (SHG) [1]. The cascading nonlinear phase shift accumulated on a short pulse induces an effective self-phase modulation similar to the cubic (Kerr) nonlinearity. Because the sign and the magnitude of the cascading nonlinearity are controllable, soliton propagation and pulse compression can be achieved in normal and anomalous dispersions [2].

The group velocity (GV) mismatch between the FF and second harmonic (SH) pulses distorts the temporal profile of the nonlinear phase shift, degrading the pulse compression performance. Another approach to suppressing such phase distortion is to exploit the large phase-mismatch condition at the expense of nonlinearity. Pulse compression of an FF pulse with a centre wavelength of 800 nm has been demonstrated by using the self-defocusing cascading nonlinearity under a large phase mismatch condition and material normal dispersion [3,4]. The few-cycle pulse compression has also been achieved via cascading nonlinearity in the stationary regime, where the effect of a GV mismatch could be considered a perturbation [5–7]. The pulse compression by using self-defocusing nonlinearity is advantageous because of its scalability to high-energy pulses.

The optical soliton in quadratic nonlinear media is intrinsically multi-colored [1,8]. Cascaded parametric interactions between the FF and SH pulses modulate their amplitude and phase in a nonlinear manner, leading to mutual trapping as well as compensation for dispersive broadening. Excitation of temporal soliton from a broader pulse is a powerful way to obtain compressed multi-colored pulses with excellent pulse quality. A frequently encountered issue in exciting a quadratic temporal soliton is the GV mismatch, which disturbs the mutual trapping between the FF and SH pulses. Temporal solitons in $\chi^{(2)}$ media were first observed by utilizing the achromatic phase-matching (APM) technique with birefringence phase matching crystal, where the GV mismatch was compensated by the interplay between the pulse-front tilting and spatial walk-off [9,10].

Engineering the evolution of quadratic soliton toward higher efficiency, higher quality factor, shorter temporal durations, etc. is a next step of significant importance. Recent developments in the GV matching scheme available with QPM devices [11,12] can open the way to the engineerable excitation of quadratic temporal solitons. Unique material dispersion of 5 mol% MgO-doped $LiNbO_3$ provides a GV matching condition for the collinear QPM-SHG configuration via an off-diagonal nonlinear coefficient $d_{32}$ at the fundamental wavelength of 1560 nm [11]. This configuration provides a condition that is preferable for temporal soliton engineering: there is no spatial or temporal walk-off, the material GVD is moderate at FF and SH frequencies and the spatial distribution of the phase mismatch profile along propagation can be arbitrarily designed.

#113385 - $15.00 USD Received 8 Jul 2009; revised 16 Aug 2009; accepted 1 Sep 2009; published 8 Sep 2009

By applying this GV matching condition to the cascaded quadratic interactions, the FF and SH pulses were compressed to about 35 fs in a 10-mm-long periodically poled MgO-doped lithium niobate (PPMgLN) device [13]. However, a large amount of energy dissipated into the pedestals because the pulse shaping process was non-adiabatic. As a scheme to avoid such pedestals, we demonstrated the adiabatic compression of femtosecond quadratic solitons in a chirped QPM grating [14,15]. The two-colored pulses in $\chi^{(2)}$ media tend to adapt to being the soliton solution, which is determined by the local effective wave-vector mismatch [16]. The SH energy increases and the temporal duration of the FF or SH pulses shorten along the propagation. The adiabatic process requires that the grating period changes only gradually along the propagation. As the interaction lengthens, however, the compressed pulses depend on the propagation distance due to diffraction.

In this paper, we study engineerable generation of quadratic temporal soliton, which is very important in view of its application in ultra-short pulse control. We show numerically that a temporal soliton with a shorter duration is efficiently excited through the seeded SHG interaction in a segmented QPM device. A SH seed pulse is generated in the first grating, and then the two-colored soliton is formed in the second grating. An appropriate phase shift induced between the FF and SH pulses mitigates the oscillating energy exchange, thus suppressing energy dissipation into a continuum. Our numerical results confirmed the advantages of the SH seeding in exciting a quadratic temporal soliton: (i) it enables the excitation of a soliton in a broad bandwidth of the wave-vector mismatch, and (ii) the compressed FF and SH pulses have spatio-temporal, high-quality profiles. The demonstrated scheme is useful for generating the timing-locked, multi-colored short pulses that have applications in optical information processing, pump-probe measurements, and light-matter control.

## 2. Soliton formation in a segmented QPM device

A schematic diagram of soliton formation in a segmented QPM device is shown in Fig. 1. The device has three parts: (i) a periodic QPM grating for SHG, (ii) a single domain for phase shift, and (iii) another periodic QPM grating for soliton evolution. The SH pulse, generated in the first grating, works as a seed in the cascaded up-and-down conversions in the second grating. Inside the $\chi^{(2)}$-grating, the effective wave-vector mismatch between FF and SH waves is $\Delta k(z) = k_2 - 2k_1 - 2\pi/\Lambda(z)$, where $\Lambda(z)$ is the QPM period and $k_1$ and $k_2$ are the FF and SH wave numbers, respectively.

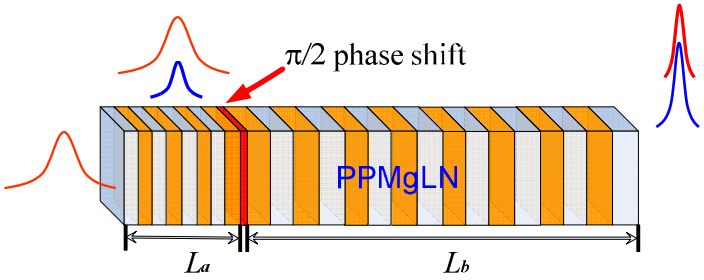


Fig. 1. (color online) A schematic of the two-colored soliton excitation in a segmented QPM structure.

The first grating with a period of $\Lambda_0$ and an interaction length of $L_a$ satisfies the QPM condition for SHG. Under the QPM condition, the SH wave generated from a nonlinear polarization and the propagating SH wave are in-phase. In contrast, the FF wave generated from nonlinear polarization and the propagating FF wave are out-of-phase. Therefore, the energy flows from the FF to the SH. A single domain with a length of $\Lambda_0/4$ is sandwiched between the segmented QPM gratings. The direction of its spontaneous polarization is reversed from that of the adjacent domains. The role of the single domain is to shift the relative phase between FF and SH pulses by $\pi/2$. Thus the FF and SH seeds are in-phase at the entrance of the second grating: The positive or negative peak of the oscillating FF field

#113385 - $15.00 USD Received 8 Jul 2009; revised 16 Aug 2009; accepted 1 Sep 2009; published 8 Sep 2009

temporally matches the positive peak of the SH field. This phase relationship suppresses the net energy exchange between the FF and SH, leading to the stationary propagation (or the excitation of solitary wave). It has been shown that the weak SH seed can control the excitation of spatial solitons in $KTiOPO_4$ (KTP) [17] and in periodically poled KTP [18]. Carrasco et al. reported that the excitation efficiency of a quadratic soliton depends strongly on the phase delay between the FF and SH: Improved excitation efficiency and broadened mismatch bandwidth are achieved with in-phase FF and SH waves [19]. In this paper, we take advantage of the in-phase SH-seeding in exciting the two-colored temporal soliton. We consider that the FF pulse at the center wavelength of 1560 nm is incident into a 10-mm-long segmented PPMgLN crystal. Nonlinear interaction via an off-diagonal component $d_{32}$ ($e$: $o$ + $o$) satisfies the GV matching condition for SHG.

The propagation of an ultra-short pulse in a quadratic nonlinear material is expressed by the (3 + 1)D (1-temporal and 2-spatial plus 1-propagation axis) model, which takes into account quadratic and cubic nonlinearities, dispersion, and diffraction. Under the slowly varying envelope approximation, the coupled wave equations governing the propagation of the FF and SH waves are generalized as [20]:

$$\begin{aligned}\left[\partial_z - i\left(1/2k_0\right)\nabla_\perp^2 + i\left(k_\omega''/2\right)\partial_{tt}^2\right]E_1 &= i\rho_1(z)E_1^* E_2\, e^{i\Delta k_0 z} + i\sigma_1\left[\left|E_1\right|^2 E_1 + 2\left|E_2\right|^2 E_1\right] \\ \left[\partial_z - i\left(1/2k_0\right)\nabla_\perp^2 + i\left(k_{2\omega}''/2\right)\partial_{tt}^2\right]E_2 &= i\rho_2(z)E_1^{\,2}\, e^{-i\Delta k_0 z} + i\sigma_2\left[\left|E_2\right|^2 E_2 + 2\left|E_1\right|^2 E_2\right]\end{aligned} \quad (1)$$

where $E_i$ ($x$, $y$, $z$, $t$) is the complex amplitude of the electric field, $\nabla_\perp^2 = \partial_{xx}^2 + \partial_{yy}^2$ is the transverse spatial Laplacian, $\rho_i$ and $\sigma_i$ involve quadratic and cubic nonlinearities, respectively, as $\rho_i(z) = \omega_i d_{32} d(z)/cn_i$ and $\sigma_i = 3\omega_i\chi^{(3)}/8cn_i$. The subscripts 1 and 2 correspond to the FF and SH pulses. Time $t$ is measured in a frame of reference moving at the GV of the FF or SH pulses. The group velocity dispersion (GVD) $k_{i\omega}'' = d^2k_{i\omega}/d^2\omega$ and the material wave-vector mismatch $\Delta k_0 = k_{2\omega} - 2k_\omega$ are derived from Sellmeier's equation for MgO: LN [21]. Here we use $d_{32}$ to be 3.4 pm/V [22] and $\chi^{(3)}$ to be $17.2 \times 10^{-22}\mathrm{m}^2/\mathrm{V}^2$ [23]. $d(z) = \pm 1$ is the normalized distribution function of the nonlinear susceptibility along the device.

### 3. Numerical results and discussions

We performed numerical simulations with the (1 + 1)-dimensional (1-temporal and 1-propagation axis) symmetric split-step beam-propagation method (BPM), neglecting the spatial diffraction effects. An input FF pulse is transform-limited with a full width at half-maximum (FWHM) duration of 100 fs (peak intensity: 20 GW/cm$^2$). The grating length and the effective wave-vector mismatch for each QPM grating are taken as $L_a$ = 0.7 mm, $\Delta k_1$ = 0 mm$^{-1}$ and $L_b$ = 9.3 mm, $\Delta k_2$ = 0 mm$^{-1}$, respectively. The QPM period satisfying $\Delta k$ = 0 mm$^{-1}$ is $\Lambda_0$ = 20.40 μm.

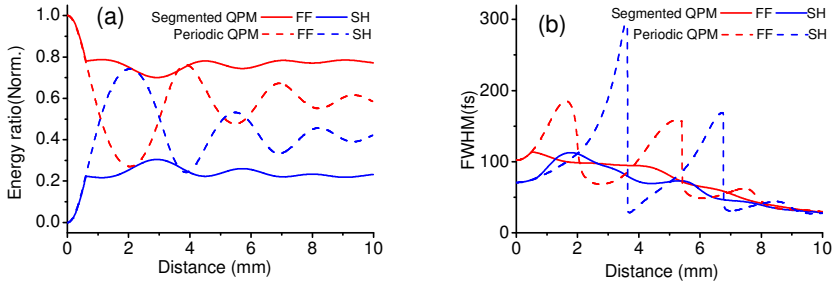


Fig. 2. (color online) (a) Normalized energy ratio and (b) pulse duration of FF (red solid and dash lines) and SH (blue solid and dash lines) pulses along propagation. The segmented QPM grating: $L_a$ = 0.7 mm ($\Delta k_1$ = 0) and $L_b$ = 9.3 mm ($\Delta k_2$ = 0); periodic QPM grating $L$ = 10 mm ($\Delta k_2$ = 0.35 mm$^{-1}$); Input FF: transform-limited pulse of 100 fs duration and 20 GW/cm$^2$ peak intensity with the center wavelength of 1560 nm.

#113385 - $15.00 USD Received 8 Jul 2009; revised 16 Aug 2009; accepted 1 Sep 2009; published 8 Sep 2009

The energy ratio and pulse duration of the FF and SH pulses along propagation are shown in Figs. 2(a) and (b), respectively. For comparison, the results for the single periodic QPM grating with $\Delta k$ = 0.35 mm$^{-1}$ and $L$ = 10 mm are also shown. This value of $\Delta k$ = 0.35 mm$^{-1}$was chosen because it gives the maximum compression factor for the interaction length of 10 mm at the input peak intensity of 20 GW/cm$^2$ [14]. The impact of the SH seeding in the soliton formation is more clearly visualized in Figs. 3 (a-d), which display the evolution of the temporal intensity profiles of (a, c) FF and (b, d) SH pulses for (a, b) the periodic QPM and (c, d) the segmented QPM gratings, respectively. In the figures, it is clear that strong oscillation in the energy exchange and in the FF and the SH pulse durations are greatly alleviated for the segmented QPM grating. The durations of the FF and SH pulses in the segmented grating shorten as propagating in an adiabatic way.

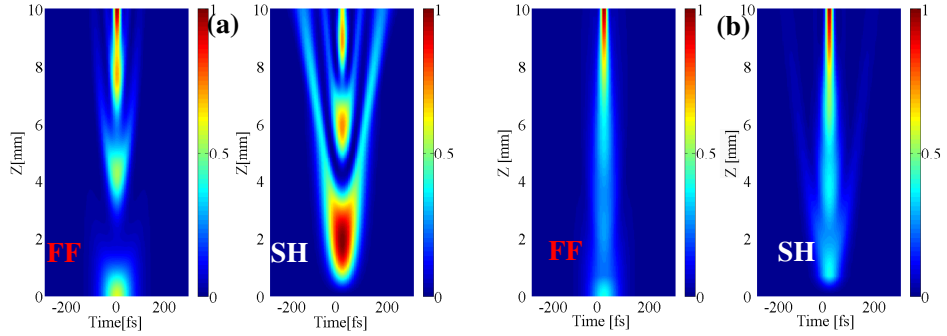


Fig. 3. (color online) Evolutions of the temporal intensity profiles of FF and SH pulses in (a) periodic and (b) segmented QPM gratings.

Figures 4(a) and (b) show the intensity profiles of the input FF, output FF, and SH pulses for each device. The FF and SH pulses are compressed to about 35 fs in both cases. The major difference is the pulse qualities of the SH pulse: The pedestal is much less for the segmented grating. In this way, the two-colored temporal soliton can be excited with less radiation into the continuum by using the segmented QPM device.

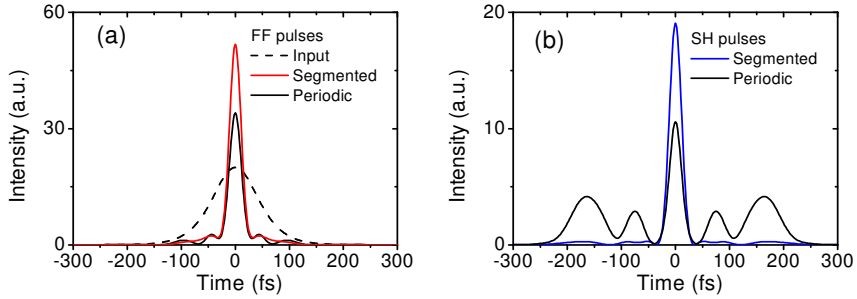


Fig. 4. (color online) Intensity profiles of the compressed (a) FF and (b) SH pulses in the segmented and periodic QPM grating.

#113385 - $15.00 USD Received 8 Jul 2009; revised 16 Aug 2009; accepted 1 Sep 2009; published 8 Sep 2009

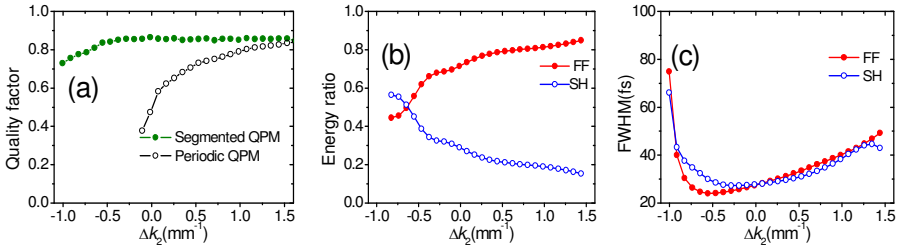


Fig. 5. (color online) (a) Quality factors for the segmented (green filled markers) and periodic (black open markers) QPM gratings, (b) normalized energy ratio and (c) pulse duration of FF (red filled) and SH (blue open) as a function of $\Delta k_2$ for the segmented QPM grating (or $\Delta k$ for the periodic QPM grating).

We evaluated the quality of compressed pulses by using the quality factor, which is defined as the fractional amount of energy carried by the central spike of the FF and SH pulses, normalized by the launched FF energy [14]. Figure 5(a) shows the quality factor as a function of $\Delta k$ for the periodic QPM grating and $\Delta k_2$ for the segmented QPM device. About 85% of the launched FF energy is contained in the central spike in a broad range of $\Delta k_2$ for the segmented QPM grating. On the other hand, the quality factor achieved in the periodic QPM grating becomes deteriorated as $\Delta k$ approaches negative values. In general, we observed pulse broadening rather than compression at negative $\Delta k$ in the periodic grating. As shown in Figs. 5 (b) and (c), the energy ratio and pulse durations of the output FF and SH calculated for the segmented device varies with $\Delta k_2$. These behaviors are consistent with the dependence of a quadratic soliton on the wave-vector mismatch. Pulse narrowing occurs both at positive and negative signs of $\Delta k_2$ because the self-defocusing nonlinearity is induced [15]. In the presence of both FF and SH waves, the nonlinear phase shift can be either positive or negative even at negative $\Delta k_2$, depending on the phase relationship between FF and SH waves.

#113385 - $15.00 USD Received 8 Jul 2009; revised 16 Aug 2009; accepted 1 Sep 2009; published 8 Sep 2009

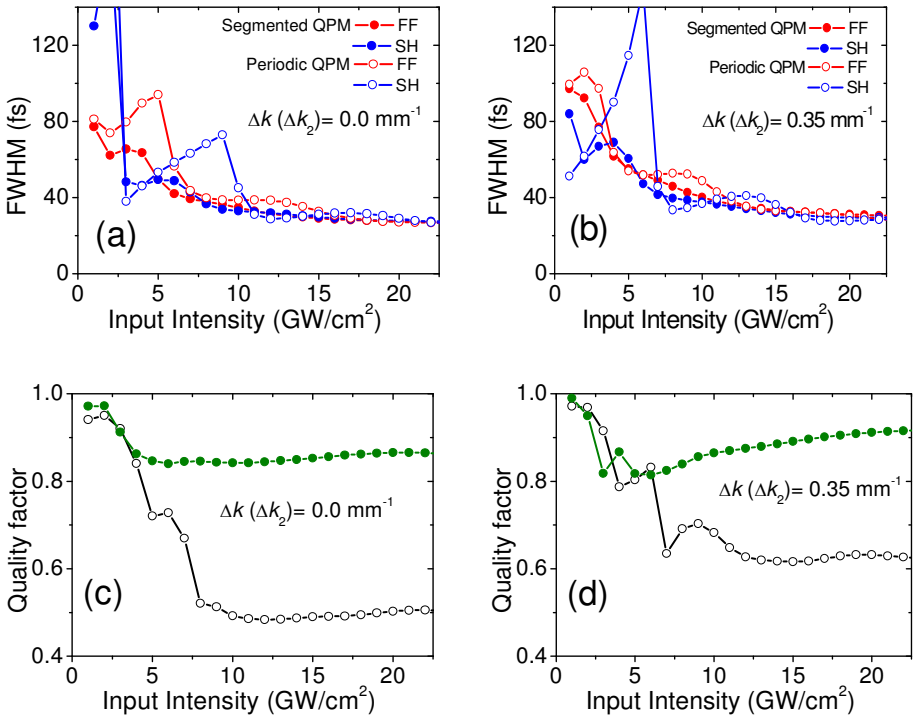


Fig. 6. (color online) Dependence of the output pulse durations (FF: red and SH: blue) on the input FF intensity for the segmented (filled) and periodic (open) gratings under the condition of (a) $\Delta k$ ($\Delta k_2$) = 0 mm$^{-1}$ and (b) 0.35 mm$^{-1}$; the quality factor for the segmented (green markers) and periodic (black markers) gratings as a function of input intensity for $\Delta k$ ($\Delta k_2$) = 0 mm$^{-1}$ and 0.35 mm$^{-1}$.

Figures 6 (a) and (b) show the dependence of the output pulse durations on the input FF intensity for the segmented and periodic gratings under the conditions of $\Delta k$ ($\Delta k_2$) = 0 mm$^{-1}$ and 0.35 mm$^{-1}$, respectively. In the case of the segmented grating, the FF and SH pulse durations decrease with intensity, without oscillatory behavior. In the case of the periodic grating, however, oscillatory behavior is clearly observed, even for input intensities higher than 10 GW/cm$^2$. Figures 6 (c) and (d) show the quality factor as a function of input intensity for $\Delta k$ ($\Delta k_2$) = 0 mm$^{-1}$ and 0.35 mm$^{-1}$. The filled green markers are for the segmented grating and the black open markers are for periodic grating. Here, the increase in the input intensity does not significantly improve the quality factor. Thus, the quality factor for the segmented grating is much larger at higher intensity levels, whereas the pulse durations become more similar between the segmented and periodic gratings at higher intensities.

Finally, we investigated the spatio-temporal dynamics of pulse propagation by numerically solving the (3D + 1) coupled-wave equations with 3D symmetric split-step Fourier BPM. The input Gaussian wave packet of FF is a transform-limited pulse with peak intensity of 20 GW/cm$^2$, pulse duration of 100 fs and the center wavelength of 1560 nm. The FF pulse is collimated to have a FWHM spatial width of 300 μm.

#113385 - $15.00 USD Received 8 Jul 2009; revised 16 Aug 2009; accepted 1 Sep 2009; published 8 Sep 2009

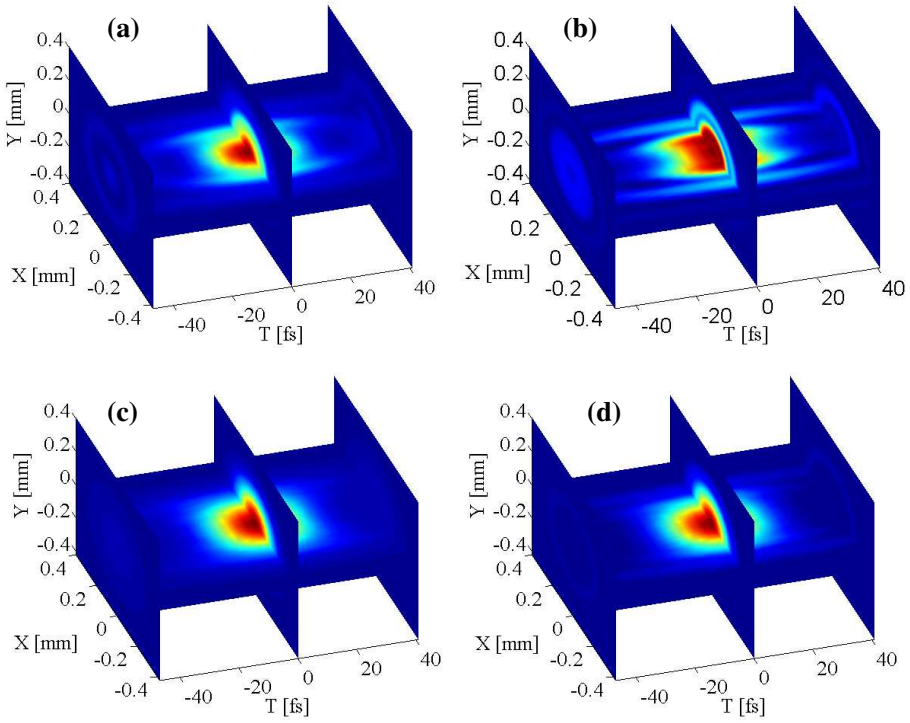


Fig. 7. (color online) 3D slices of the compressed wave packets of (a) FF and (b) SH pulses in periodic QPM grating and (c) FF and (d) SH pulses in segmented QPM grating.

Figures 7 (a-d) show the 3D slice of the spatio-temporal intensity profiles of the compressed FF and SH pulses for the periodic and segmented QPM gratings. The FF and SH pulses are compressed to around 40 fs in the segmented and periodic QPM gratings. The intensity pattern of the compressed SH in the periodic QPM grating clearly splits up into a central hump and a pedestal in the spatial and temporal domains. In contrast, only a single central hump is observed in the spatio-temporal intensity profile of the FF or SH pulses for the segment QPM grating. The improved spatio-temporal profile (i.e., less radiation into the continuum) results from the suppressed oscillation during the energy exchange, which is brought about by the in-phase SH-seeding.

## 4. Conclusions

We have numerically investigated the excitation of a two-colored temporal soliton in a segmented QPM device. The SH seed generated in the first QPM grating can be used to control the cascaded second-order nonlinear interactions in the second grating: A quadratic temporal soliton was adiabatically shaped in the second grating by the in-phase SH seeding. Numerical results show that the segmented QPM device, taking advantage of the in-phase SH-seeding, enables the excitation of a two-colored soliton with a higher quality factor in a broader wave-vector range, compared with the periodic QPM grating of the same device length.

## Acknowledgements

This work is supported in part by the Natural Science Foundation of China (10704047 and 10874120), Shanghai Leading Academic Discipline Project and STCSM (S30108 and 08DZ2231100), SRF for ROCS, SEM, Shanghai Pujiang Program (08PJ14056) and Shanghai Municipal Education Commission (08zz49). Xianglong Zeng's email address is zenglong@shu.edu.cn.

#113385 - $15.00 USD Received 8 Jul 2009; revised 16 Aug 2009; accepted 1 Sep 2009; published 8 Sep 2009